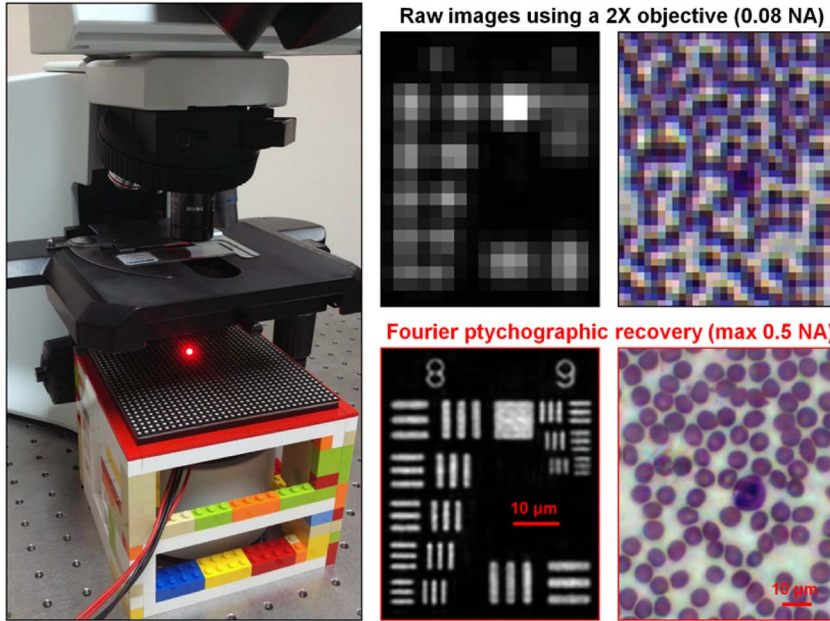


# Breakthroughs in Photonics 2013: Fourier Ptychographic Imaging

Volume 6, Number 2, April 2014

Guoan Zheng



---

DOI: 10.1109/JPHOT.2014.2308632  
1943-0655 © 2014 IEEE

# Breakthroughs in Photonics 2013: Fourier Ptychographic Imaging

Guoan Zheng

(Invited Paper)

Biomedical Engineering, University of Connecticut, Storrs, CT 06269-3247 USA  
Electrical and Computer Engineering, University of Connecticut, Storrs, CT 06269-2157 USA

DOI: 10.1109/JPHOT.2014.2308632

1943-0655 © 2014 IEEE. Translations and content mining are permitted for academic research only.  
Personal use is also permitted, but republication/redistribution requires IEEE permission.  
See [http://www.ieee.org/publications\\_standards/publications/rights/index.html](http://www.ieee.org/publications_standards/publications/rights/index.html) for more information.

Manuscript received February 9, 2014; accepted February 19, 2014. Date of publication March 3, 2014; date of current version April 30, 2014. Corresponding author: G. Zheng (e-mail: guoan.zheng@uconn.edu).

**Abstract:** Fourier ptychography (FP) is a recently developed computational framework for high-resolution high-throughput imaging. In this paper, we will review the latest development of the Fourier ptychographic imaging scheme. We will demonstrate its applications in wide-field imaging, quantitative phase imaging, and adaptive imaging. We will also discuss its potential applications in X-ray optics and transmission electron microscopy.

**Index Terms:** Coherent imaging, imaging systems, microscopy.

## 1. Introduction

Resolution of conventional imaging platforms is in general limited by the numerical aperture (NA) of the objective lens. Improving resolution beyond the cut-off frequency of the objective lens has been a long-standing goal in the research community. In recent years, there have been intensive research efforts on applying the synthetic aperture technique (originally developed for radio astronomy [1]) to achieve this goal [2]–[8]. Synthetic aperture technique stitches many complex measurements in the Fourier space to expand the passband and improve the achievable resolution. The reconstruction process of this technique, however, requires the knowledge of both the intensity and phase information of the incoming light field. Therefore, most implementations employ delicate interferometry setups for complex light field recording and precise mechanical actuations for incident beam scanning. It has been shown that the resolution improvement beyond the NA of the underlying optical systems is possible through such a computational data fusion process [2]–[8].

Recently, we have developed an imaging approach that extends the concept of synthetic aperture imaging for non-interferometry setups. The reported approach, termed Fourier ptychography (FP) [9], iteratively stitches together many variably illuminated, low-resolution intensity images in the Fourier space to expand the frequency passband and recover a high-resolution complex sample image. Instead of directly measuring the phase information of the incoming light field, FP uses an iterative phase retrieval process to recover the complex phase information of the sample. It has been shown that [9], without involving any interferometry measurement and mechanical scanning, FP facilitates microscopic imaging well beyond the cutoff frequency set by the NA of the objective lens.

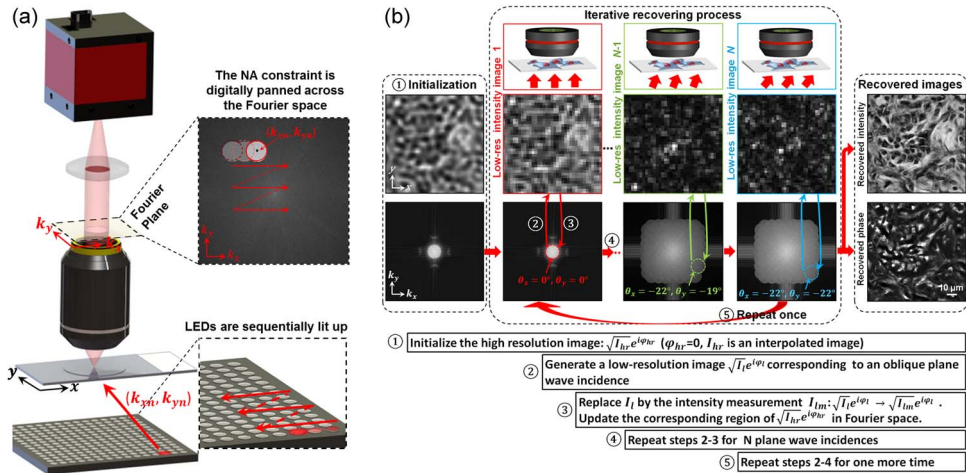


Fig. 1. The FP setup and the recovery procedures (adapted from [9] and [11]). (a) An LED array is used to illuminate the sample with angle-varied plane waves. The objective's optical-transfer-function imposes a well-defined constraint in the Fourier domain. This constraint is digitally panned across the Fourier space to reflect the angular variation of angle-varied illuminations. (b) The iterative phase retrieval procedures of the FP.

## 2. Fourier Ptychography: Scheme and Principle

A typical FP platform consists of an LED array and a conventional microscope with a low-NA objective lens, as shown in Fig. 1(a). The LED array is used to successively illuminate the sample at different incident angles (one LED element corresponds one incident angle). At each illumination angle, FP records a low-resolution intensity image of the sample. Under the thin-sample assumption, each acquired image uniquely maps to a different passband of the sample's spectrum. The FP algorithm then recovers a high-resolution complex sample image by alternatively constraining its amplitude to match the acquired low-resolution image sequence, and its spectrum to match the panning Fourier constraint, as shown in Fig. 1(a). Essentially, FP introduces angular diversity functions to recover the high-resolution complex sample image, as compared to the translational diversity functions used in the conventional ptychography approach [10].

The reconstruction procedures of the FP are shown in Fig. 1(b). It starts with a high-resolution spectrum estimate of the sample:  $\hat{U}_0(k_x, k_y)$ . This sample spectrum estimate is then sequentially updated with the low-resolution intensity measurements  $I_{mi}$  (subscript "m" stands for measurement and "i" stands for the  $i^{\text{th}}$  LED). For each update step, we select a small sub-region of the  $\hat{U}_0(k_x, k_y)$ , corresponding to the optical-transfer-function of the objective lens, and apply Fourier transformation to generate a new low-resolution target image  $\sqrt{I_{li}} e^{i\varphi_{li}}$  (subscript "l" stands for low-resolution and "i" stands for the  $i^{\text{th}}$  LED). We then replace the target image's amplitude component  $\sqrt{I_{li}}$  with the square root of the measurement  $\sqrt{I_{mi}}$  to form an updated, low-resolution target image  $\sqrt{I_{mi}} e^{i\varphi_i}$ . This image is then used to update its corresponding sub-region of  $\hat{U}_0(k_x, k_y)$ . The replace-and-update sequence is repeated for all intensity measurements, and we iterate through the above process several times until solution convergence, at which point  $\hat{U}_0(k_x, k_y)$  is transformed to the spatial domain to produce a high-resolution complex sample image. The achievable resolution of the final FP reconstruction is determined by the latest incident angle of the LED array. As such, FP is able to bypass the design conflicts of conventional microscopes to achieve high-resolution, wide field-of-view imaging capabilities.

The name of 'Fourier ptychography' comes from a related phase retrieval scheme, ptychography [10], [12]–[23]. Ptychography is lensless imaging approach originally proposed for transmission electron microscopy [12] and brought to fruition by Faulkner and Rodenburg [13]. It uses a focused beam to illuminate the sample and records multiple diffraction patterns as a function of sample positions. This set of diffraction patterns is then used to invert the diffraction process and recover the complex sample profile following the iterative phase retrieval strategy. It is clear that FP and

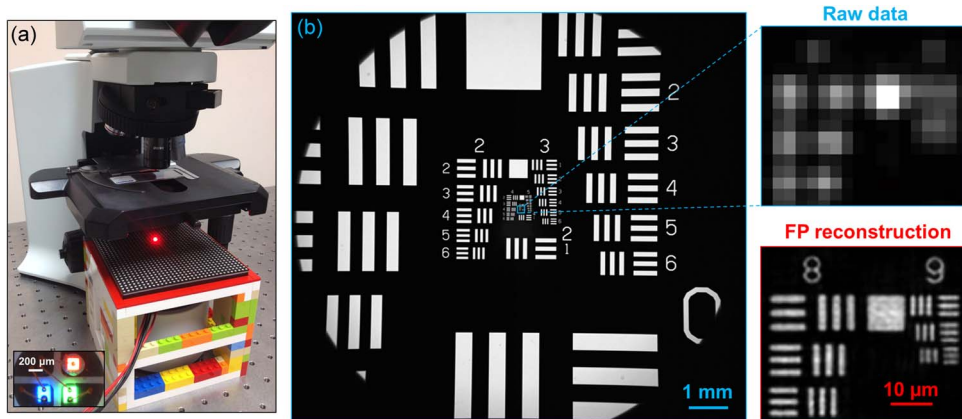


Fig. 2. Wide-field, high-resolution imaging via FP (adapted from [9]). FP combines the field-of-view advantage of a 2X objective and resolution advantage of a 20X objective.

ptychography both share the strategy of phase retrieval technique: iteratively seeking a complex sample solution that is consistent with many intensity measurements. With ptychography, the object support constraints for phase retrieval are imposed by the confined illumination beam in the spatial domain. As such, the sample must be mechanically scanned through the desired field-of-view. With FP, on the other hand, the object support constraints are given by the confined optical-transfer-function in the Fourier domain. In this regard, FP acts as the Fourier counterpart to ptychography, justifying its name [24]. By using a low-NA objective lens, FP naturally offers a large and fixed field-of-view, high signal-to-noise ratio, and no mechanical scanning as compared to the conventional ptychography. The use of lens elements in FP settings also reduces the coherence requirement of the light source. Post-processing used in conjunction with the panning LED illuminations then leads to a resolution-improved, high-pixel-count final image. Furthermore, as discussed below, FP is able to digitally correct for aberrations and extend the depth-of-focus beyond the physical limitation of the objective lens.

### 3. Imaging Applications Using Fourier Ptychography

The unique computational scheme of FP enables many applications for microscopy imaging. In this section, we will review the recent developments of FP for wide-field imaging, quantitative phase imaging, and adaptive imaging.

#### 3.1. Wide-Field, High-Resolution, Long Depth-of-Focus Imaging

Physical limitations of the objective lens have forced researchers to decide between high-resolution and a small field-of-view on one hand, or low-resolution and a large field-of-view on the other. That has meant that scientists have either been able to see a lot of detail very clearly but only in a small area, or they have gotten a coarser view of a much larger area. FP, on the other hand, decouples the resolution from the employed optics, and as such, it is able to achieve high-resolution and wide field-of-view at the same time.

We have demonstrated the use of a 2X objective lens to achieve the resolution of a 20X objective lens [9]. Therefore, FP combines the field-of-view advantage of a 2X objective lens and the resolution advantage of a 20X objective lens, as shown in Fig. 2. The final image produced by FP contains orders of magnitude more information than that of conventional microscope platforms. Fig. 3 demonstrates the raw FP image, FP reconstructions and images using conventional objective lens. We can see that the image quality of the FP reconstructions is comparable to that of the conventional high-NA objective lens. Furthermore, a phase factor can be introduced in the FP recovery procedures to correct for various aberrations of the objective lens. We have shown that, such a phase-factor correcting method enables FP to correct for defocus aberration and extend the depth-of-focus to 0.3 mm, two orders of magnitude longer than that of the conventional platform with a similar NA [9].

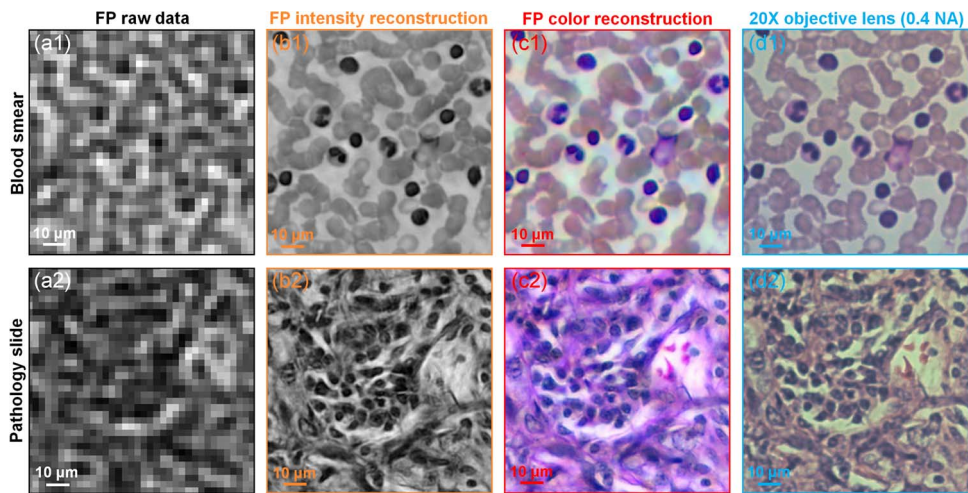


Fig. 3. Comparisons between raw data, high-resolution FP constructions and images captured by high-NA objective (adapted from [9]).

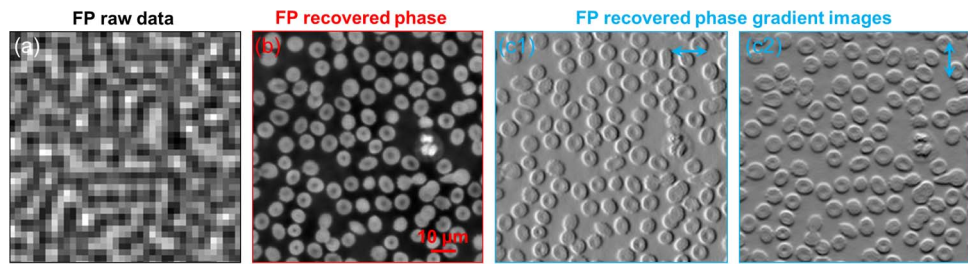


Fig. 4. Quantitative phase and phase gradient imaging via FP (adapted from [11]). (a) FP raw data. (b) FP recovered phase image. (c) FP generated phase gradient images, simulating the appearance of conventional DIC microscopes.

The wide-field, high-resolution, long depth-of-focus imaging capability offered by FP is in particular useful for digital pathology and hematology applications. This technique may potentially free clinicians from bowing in front of the microscope and manually moving the sample to different regions for observation. As digital imaging is introduced to laboratory environment, it may also have the potential to improve the work environment and laboratory productivity, to enable education, and to enhance communication and collaboration between clinicians.

### 3.2. Quantitative Phase Imaging

Many biological samples do not absorb or scatter light significantly. As such, they are transparent or generate little contrast under a conventional bright-field microscope. To address this problem, phase contrast and differential-interference-contrast microscopes have been developed to convert the phase delay information into intensity variations, and these two types of microscopes have been widely used in biological laboratories to visualize live cell samples. However, the phase information generated by these two types of microscopes are mixed with the intensity information, and thus, it is not quantitative in nature.

As discussed in Section 2, FP is able to recover both the intensity and phase of an optical field exiting a sample. We have shown that, the phase information recovered by the FP approach is quantitative in nature [11]. Therefore, it holds a great potential for quantitative image analysis. Furthermore, the use of low-coherent LED in FP settings suppresses coherent noise sources such as speckle noise. Fig. 4(a) and (b) demonstrate the raw data and the FP recovered phase image.

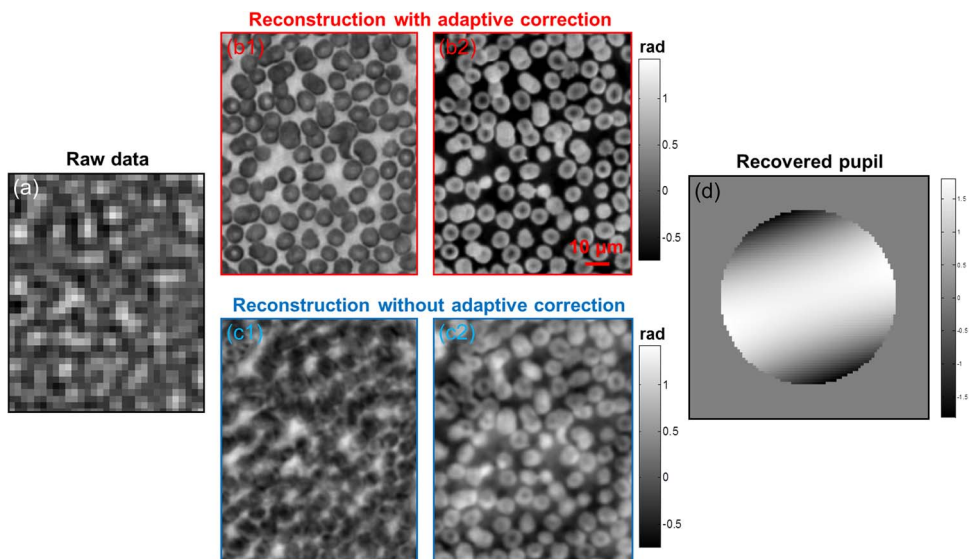


Fig. 5. (a) FP raw data. (b) Reconstructions using the adaptive FP scheme. (c) Reconstructions without using the adaptive FP scheme. (d) The recovered pupil function using the adaptive FP scheme. (adapted from [28]).

The FP recovered phase can be further processed to generate the phase gradient images, as shown in Fig. 4(c1) and (c2). The generated phase gradient images simulate the improved visibility of a differential-interference-contrast (DIC) microscopy; however, they are quantitative in nature as compared to the DIC microscopy.

### 3.3. Adaptive Fourier Ptychographic Imaging

The concepts in adaptive optics [25]–[27] can also be implemented in the FP scheme to perform adaptive Fourier ptychographic imaging [28]. In the adaptive FP scheme, an image-quality metric is defined as a guide star for the optimization process, and system corrections are then performed to maximize such a guide star. Compared to conventional adaptive imaging systems, the adaptive FP scheme performs system corrections by modifying the complex transfer function in the iterative recovery process (no adaptive optical hardware is needed), offering a unique advantage on system simplicity and reliability. Fig. 5 demonstrates the use of the adaptive FP to recover the unknown pupil function and perform aberration correction. Such a scheme can also be used to correct for intensity uncertainty of the LED array and recover unknown system parameters [28].

## 4. Discussion

It is clear that FP is a promising computational framework for microscopy imaging. It transforms the challenge of high-resolution imaging from one that is coupled to the hardware limitations to one that is solvable through computation [9]. More broadly speaking, the FP scheme can also be applied to other imaging modalities to improve the achievable resolution. We believe that FP is able to improve the resolution of transmission electron microscope. To implement FP for electron imaging, one can simply use the magnetic deflection coils in most existing electron microscopes to shift the incident angle of the electron beam. Compared to conventional lensless ptychography, the use of focusing element in FP settings also provides a higher signal-to-noise ratio and reduces the requirement of spatial coherence of the electron beam. Following a similar logic, FP may also be useful for X-ray microscopy. The sample and the detector can be placed on a rotating stage to record intensity patterns corresponding to different incident angles. The phase-factor correction scheme in FP can be used to correct for aberrations of the X-ray optics.

Finally, it is also important to discuss the limitations of the FP approach. First, current FP algorithms are designed for 2D thin samples. However, it is possible to integrate the FP concept with tomographic imaging approaches [29]–[32] for 3D high-resolution imaging. Second, the FP approach is a coherent imaging technique, and thus, it is not suited for fluorescent imaging. Third, the throughput of current FP prototypes is limited by the low light intensity of the LED array. This issue can be addressed by using a high-power LED array.

## References

- [1] M. Ryle and A. Hewish, "The synthesis of large radio telescopes," *Mon. Not. R. Astron. Soc.*, vol. 120, p. 220, 1960.
- [2] V. Mico, Z. Zalevsky, and J. García, "Superresolution optical system by common-path interferometry," *Opt. Exp.*, vol. 14, no. 12, pp. 5168–5171, Jun. 2006.
- [3] J. García, Z. Zalevsky, and D. Fixler, "Synthetic aperture superresolution by speckle pattern projection," *Opt. Exp.*, vol. 13, no. 16, pp. 6073–6078, Aug. 2005.
- [4] V. Mico, Z. Zalevsky, P. García-Martínez, and J. García, "Synthetic aperture superresolution with multiple off-axis holograms," *J. Opt. Soc. Amer. A. Opt. Image sci.*, vol. 23, no. 12, pp. 3162–3170, Dec. 2006.
- [5] V. Mico, Z. Zalevsky, P. García-Martínez, and J. García, "Single step superresolution by interferometric imaging," *Opt. Exp.*, vol. 12, no. 12, pp. 2589–2596, Jun. 2004.
- [6] S. A. Alexandrov, T. R. Hillman, T. Gutzler, and D. D. Sampson, "Synthetic aperture Fourier holographic optical microscopy," *Phys. Rev. Lett.*, vol. 97, no. 16, pp. 168102-1–168102-4, Oct. 2006.
- [7] J. Di, J. Zhao, H. Jiang, P. Zhang, Q. Fan, and W. Sun, "High resolution digital holographic microscopy with a wide field of view based on a synthetic aperture technique and use of linear CCD scanning," *Appl. Opt.*, vol. 47, no. 30, pp. 5654–5659, Oct. 2008.
- [8] T. R. Hillman, T. Gutzler, S. A. Alexandrov, and D. D. Sampson, "High-resolution, wide-field object reconstruction with synthetic aperture Fourier holographic optical microscopy," *Opt. Exp.*, vol. 17, no. 10, pp. 7873–7892, May 2009.
- [9] G. Zheng, R. Horstmeyer, and C. Yang, "Wide-field, high-resolution Fourier ptychographic microscopy," *Nat. Photon.*, vol. 7, no. 9, pp. 739–745, Sep. 2013.
- [10] M. Guizar-Sicairos and J. R. Fienup, "Phase retrieval with transverse translation diversity: A nonlinear optimization approach," *Opt. Exp.*, vol. 16, no. 10, pp. 7264–7278, May 2008.
- [11] X. Ou, R. Horstmeyer, C. Yang, and G. Zheng, "Quantitative phase imaging via Fourier ptychographic microscopy," *Opt. Lett.*, vol. 38, no. 22, pp. 4845–4848, Nov. 2013.
- [12] W. Hoppe and G. Strube, "Diffraction in inhomogeneous primary wave fields. 2. Optical experiments for phase determination of lattice interferences," *Acta Crystallogr. A. Found. Crystallogr.*, vol. 25, pp. 502–507, 1969.
- [13] H. M. L. Faulkner and J. M. Rodenburg, "Movable aperture lensless transmission microscopy: A novel phase retrieval algorithm," *Phys. Rev. Lett.*, vol. 93, no. 2, pp. 023903-1–023903-4, Jul. 2004.
- [14] P. Thibault, M. Dierolf, A. Menzel, O. Bunk, C. David, and F. Pfeiffer, "High-resolution scanning X-ray diffraction microscopy," *Science*, vol. 321, no. 5887, pp. 379–382, Jul. 2008.
- [15] P. Thibault, M. Dierolf, O. Bunk, A. Menzel, and F. Pfeiffer, "Probe retrieval in ptychographic coherent diffractive imaging," *Ultramicroscopy*, vol. 109, no. 4, pp. 338–343, Mar. 2009.
- [16] M. Dierolf, P. Thibault, A. Menzel, C. M. Kewish, K. Jefimovs, I. Schlichting, K. von König, O. Bunk, and F. Pfeiffer, "Ptychographic coherent diffractive imaging of weakly scattering specimens," *New J. Phys.*, vol. 12, no. 3, p. 035017, Mar. 2010.
- [17] A. M. Maiden, J. M. Rodenburg, and M. J. Humphry, "Optical ptychography: A practical implementation with useful resolution," *Opt. Lett.*, vol. 35, no. 15, pp. 2585–2587, Aug. 2010.
- [18] F. Hüe, J. Rodenburg, A. Maiden, and P. Midgley, "Extended ptychography in the transmission electron microscope: Possibilities and limitations," *Ultramicroscopy*, vol. 111, no. 8, pp. 1117–1123, Jul. 2011.
- [19] A. Shenfield and J. M. Rodenburg, "Evolutionary determination of experimental parameters for ptychographical imaging," *J. Appl. Phys.*, vol. 109, no. 12, pp. 124 510–124 518, Jun. 2011.
- [20] M. Humphry, B. Kraus, A. Hurst, A. Maiden, and J. Rodenburg, "Ptychographic electron microscopy using high-angle dark-field scattering for sub-nanometre resolution imaging," *Nat. Commun.*, vol. 3, no. 3, p. 730, Mar. 2012.
- [21] T. B. Edo, D. J. Batey, A. M. Maiden, C. Rau, U. Wagner, Z. D. Peši, T. A. Waigh, and J. M. Rodenburg, "Sampling in X-ray ptychography," *Phys. Rev. A*, vol. 87, no. 5, pp. 053850-1–053850-8, May 2013.
- [22] M. Stefano, S. Andre, Y. Chao, W. Hau-tieng, and M. Filipe, "Augmented projections for ptychographic imaging," *Inverse Probl.*, vol. 29, no. 11, pp. 115 009–115 031, Nov. 2013.
- [23] J. M. Rodenburg and R. H. T. Bates, "The theory of super-resolution electron microscopy via Wigner-distribution deconvolution," *Philos. Trans. Roy. Soc. London A, Math. Phys. Sci.*, vol. 339, no. 1655, pp. 521–553, Jun. 1992.
- [24] R. Horstmeyer and C. Yang, "A phase space model of Fourier ptychographic microscopy," *Opt. Exp.*, vol. 22, no. 1, pp. 338–358, Jan. 2014.
- [25] M. J. Booth, "Adaptive optics in microscopy," *Philos. Trans. Roy. Soc. London A, Math. Phys. Sci.*, vol. 365, no. 1861, pp. 2829–2843, Dec. 2007.
- [26] D. Debarre, M. J. Booth, and T. Wilson, "Image based adaptive optics through optimisation of low spatial frequencies," *Opt. Exp.*, vol. 15, no. 13, pp. 8176–8190, Jun. 2007.
- [27] J. Fienup and J. Miller, "Aberration correction by maximizing generalized sharpness metrics," *J. Opt. Soc. Amer. A. Opt. Image Sci.*, vol. 20, no. 4, pp. 609–620, Apr. 2003.
- [28] Z. Bian, S. Dong, and G. Zheng, "Adaptive system correction for robust Fourier ptychographic imaging," *Opt. Exp.*, vol. 21, no. 26, pp. 32 400–32 410, Dec. 2013.

- [29] W. Choi, C. Fang-Yen, K. Badizadegan, S. Oh, N. Lue, R. R. Dasari, and M. S. Feld, "Tomographic phase microscopy," *Nat. Methods*, vol. 4, no. 9, pp. 717–719, Sep. 2007.
- [30] S. O. Isikman, W. Bishara, S. Mavandadi, W. Y. Frank, S. Feng, R. Lau, and A. Ozcan, "Lens-free optical tomographic microscope with a large imaging volume on a chip," *Proc. Nat. Acad. Sci. USA*, vol. 108, no. 18, pp. 7296–7301, May 2011.
- [31] G. Zheng, C. Kolner, and C. Yang, "Microscopy refocusing and dark-field imaging by using a simple LED array," *Opt. Lett.*, vol. 36, no. 20, pp. 3987–3989, Oct. 2011.
- [32] S. A. Lee, G. Zheng, N. Mukherjee, and C. Yang, "On-chip continuous monitoring of motile microorganisms on an ePetri platform," *Lab Chip*, vol. 12, no. 13, pp. 2385–2390, 2012.